SIMULATION OF PHASE TRANSITION PROCESS IN RECONSTRUCTED POROUS MEDIUM BASED ON LATTICE BOLTZMANN METHOD

by

Shouguang YAO[a]*, Luobin DUAN[a], Kai ZHAO[b], Jiangbang ZENG[c], Zheshu MA[a], and Xinwang JIA[a]

[a] Jiangsu University of Science and Technology, Zhenjiang, Jiangsu, China
[b] China International Marine Containers (Group) Co., Ltd., Nantong, Jiangsu, China
[c] School of Mechanical Engineering, East China Jiaotong University, Nanchang, China

Original scientific paper
https://doi.org/10.2298/TSCI160817007Y

At the pore scale level, 2-D porous medium structures of porous media with different porosities (isotropic) and the same porosities (anisotropic) were constructed using quartet structure generation set. A random porous cavity was selected and combined with the lattice Boltzmann model to describe the gas-liquid phase transition process. Bubble generation, growth, mutual fusion, and collision as well as rebound process in porous media framework were investigated by simulating the phase transition phenomenon in porous media. Calculation results show that in three different heat loads, the maximum relative errors between the qualities of gas phase and liquid phase and theoretical solution of gas phase were 0.09%, 0.19%, and 0.32%, respectively, whereas the values for liquid phase were 0.11%, 0.38%, and 1.49%, respectively. Simulation results coincide with the theoretical solution perfectly, verifying the accuracy and feasibility of the model for random porous structures.

Key words: *porous media, pore scale, phase transition*

Introduction

Energy, momentum and mass transfers in porous media are important factors in industrial and agricultural fields. Phase change heat transfer in porous media is a benchmark problem in a wide variety of applications, such as heat pipe, heat insulating material, petroleum reserve, groundwater decontamination, thermal drying process and casting solidification. Given the complexity of the internal structure of porous media, internal flow heat transfer is usually studied at three levels, namely, pore scale, representative elementary volume scale and macro scale. At present, scholars [1-4] have studied problems on phase change heat transfer in porous media under the condition of representative elementary volume and macro scales.

The research of this problem at pore scale level not only reflects the morphology of porous structure, but also provides full consideration to complex boundary effects of the porous media on changes in internal phase. After decades of development as a promising numerical method, lattice Boltzmann method (LBM) [5, 6] has become a tool to simulate fluid motion and model complex physical phenomena. Unlike the traditional method of computational fluid

* Corresponding author, e-mail: zjyaosg@126.com

mechanics, LBM is not based on the macroscopic continuous equation but grounded on the fluid microscopic model and mesoscopic dynamic equations. The evolution mechanism in accordance with physical laws is constructed for calculation. The LBM can be used to simulate heat and mass transfer problems in complex structures of porous media because of its simple implementation, good concurrency and simple boundary treatment.

At the pore scale, quartet structure generation set is introduced to generate random porous media. The phase change lattice Boltzmann model proposed by Zhao *et al.* [7] is combined with two different dimensional porous structures to simulate the phase change process of liquid in a porous medium. Results show the formation, growth and merging of bubbles inside the complex porous media.

Random porous media reconstruction

The spatial distribution of a porous medium can be expressed as the phase function $Z(x)$:

$$Z(x) = \begin{cases} 1, & x \quad \text{is lacated in pore internal} \\ 0, & x \quad \text{is located in the skeleton} \end{cases}$$

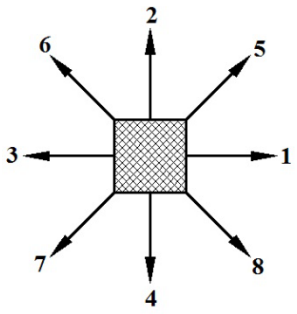

Figure 1. The QSGS growth directions

Owing to the randomness of porous media, $Z(x)$, can be thought of as a random variable. Its statistical features reflect the pore distribution characteristics, for example, the value of porosity is equal to the average $Z(x)$.

Quartet structure generation set (QSGS) by Wang *et al*. [8] is used to construct the 2-D random porous media. This method can control the generation of porous structure by adjusting the morphology parameters. The 2-D QSGS needs eight growth directions, as shown in fig. 1. Before the initialization of construction space, the growth and non-growth phases are selected. In this study, the solid area is selected as the growth phase to reconstruct the porous framework. Based on this generation method, the formation steps of porous structure are:

- Assume that the whole structure is the skeleton mesh, and arrange the generative nucleus of the initial growth phase in the grid randomly with a certain probability, P_c, which should be less than the volume fraction of the phase.
- Each initial growth nuclei grows with the probability, P_i, in direction i. For each growth volume element, a group of new random number is assigned to their adjacent nodes. If the random number of adjacent nodes is less than P_i, then this adjacent node grows as the porous framework.
- Repeat the second step until the preset volume-fraction of the porous structure is achieved.

As shown in fig. 2, different kinds of isotropic 2-D pore structure are generated according to different porosities of porous media, the base mesh is the D2Q9 lattice, with gird size of 200 × 200, and the growth directions correspond to 8 non-zero discrete velocities. The black part in the picture is the solid matrix of the growth phase, and the white part is the pore.

The porosity in the porous media map from 2(a) to 2(d) are 0.2, 0.4, 0.6, and 0.8, respectively, with $P_c = 0.01$, the P_i in each direction is 0.005. As shown in the pictures, the constructed porous media have a certain degree of similarity and authenticity compared with the real porous structure. With the increase of porosity, the framework phase is gradually reduced, whereas the connectivity of pore channel is gradually increased, as well as the connected area.

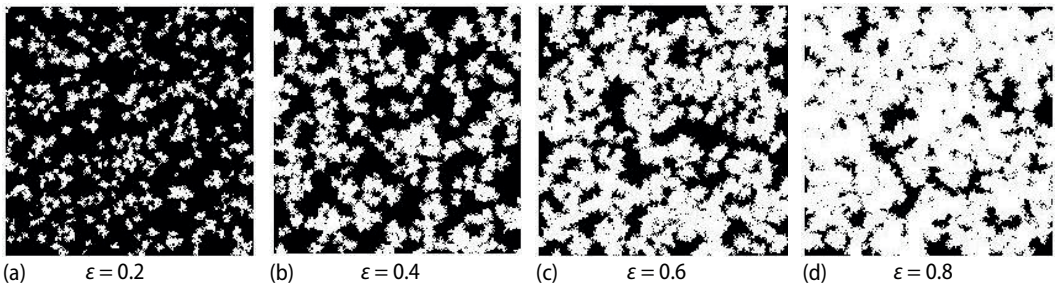

Figure 2. Pore structures of 2-D porous media with different porosities

Figure 3 shows the anisotropic porous structure, in which the parameters are: porosities are all 0.7, $P_c = 0.01$; (a) $P_i = 0.05$; (b) $P_1 = P_3 = 0.05$, other directions $P_i = 0.005$; (c) $P_2 = P_4 = 0.05$, other directions $P_i = 0.005$; and (d) $P_5 = P_7 = 0.05$, other direction $P_i = 0.005$. We can see directly from the figure that the morphology of the porous medium structure is remarkably different because of the different growth probabilities in all directions. Therefore, the QSGS method can produce porous isotropy and anisotropy conveniently by changing the direction of growth probability.

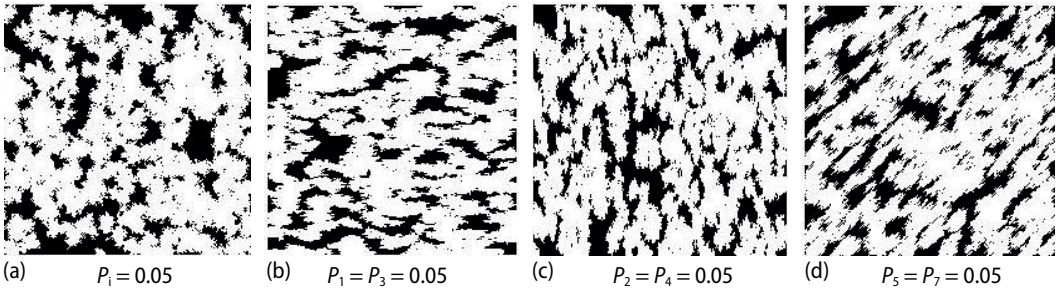

Figure 3. Pore structures of different growth directions for 2-D porous media

Phase change lattice Boltzmann model

Basic multiphase model

A theoretical model is applied to describe the gas-liquid phase change process. The evolution equations for this model can be expressed [9]:

$$f_i^{\sigma}(\boldsymbol{x}+\boldsymbol{e}_i\Delta t, t+\Delta t) - f_i^{\sigma}(\boldsymbol{x},t) = \frac{f_i^{\sigma \mathrm{eq}}(\boldsymbol{x},t) - f_i^{\sigma}(\boldsymbol{x},t)}{\tau^{\sigma}} \tag{1}$$

where $\sigma = 1,2,...S$ represents S different components, the subscript $i = 0,1,...,\mathrm{Q}$ represents the lattice velocity direction, $\boldsymbol{e}_i$ is the lattice velocity vector, and $\boldsymbol{x}$ and Δt are position vector and discrete time step, respectively. The τ^{σ} is the dimensionless collision relaxation time of the σ^{th} component of the fluid, $f_i^{\sigma}(\boldsymbol{x},t)$ is the population of the particles of σ^{th} component with velocity e_i at lattice x and time t, and $f_i^{\sigma eq}(\boldsymbol{x},t)$ is the equilibrium distribution function which is defined:

$$f_i^{\sigma\mathrm{eq}}=\begin{cases} f^{\sigma}\left[\dfrac{1-d_{\sigma}}{b}+\dfrac{D(\boldsymbol{e}_i\boldsymbol{u}_{\sigma}^{\mathrm{eq}})}{c^2b}+\dfrac{D(D+2)}{2c^4b}\boldsymbol{e}_i\boldsymbol{e}_i:\boldsymbol{u}_{\sigma}^{\mathrm{eq}}\boldsymbol{u}_{\sigma}^{\mathrm{eq}}-\dfrac{D\boldsymbol{u}_{\sigma}^{\mathrm{eq}}}{2c^2b}\right] & i=1,2,...,b \\ f^{\sigma}\left[d_{\sigma}-(\dfrac{\boldsymbol{u}_{\sigma}^{\mathrm{eq}}}{c})^2\right] & i=0 \end{cases} \tag{2}$$

where $d_\sigma < 1$ denotes to the percentage of static particles at equilibrium, $c = \Delta x/\Delta t$ – the lattice speed, D – is the space dimension, $f^{\sigma} = \sum f_i^{\sigma}$ – the density of the σ^{th} component, and $\boldsymbol{u}_{\sigma}^{\mathrm{eq}}$ – the equilibrium speed.

In a false potential model, the influence of the interaction force between particles is reflected by changing the speed of the equilibrium state in the equilibrium distribution function:

$$\rho_{\sigma}\boldsymbol{u}_{\sigma}^{\mathrm{eq}} = \rho_{\sigma}\boldsymbol{u}' + \tau_{\sigma}\boldsymbol{F}_{\sigma} \tag{3}$$

where $\rho_\sigma = m_\sigma f^{\sigma}$ is the mass density, m_σ – the molecular mass of the σ^{th} component, $\boldsymbol{F}_\sigma = \boldsymbol{F}_1 + \boldsymbol{F}_2 + \boldsymbol{F}_3$ stands for the total force of particles, $\boldsymbol{F}_1, \boldsymbol{F}_2$ and $\boldsymbol{F}_3$ are the interaction force of fluid particles, and the interaction force between fluids and solid walls and other external forces, respectively.

$$\boldsymbol{u}_{\sigma}^{\mathrm{eq}} = \boldsymbol{u}' = \frac{\sum\limits_{\sigma}\dfrac{\rho_{\sigma}\boldsymbol{u}_{\sigma}}{\tau^{\sigma}}}{\sum\limits_{\sigma}\dfrac{\rho_{\sigma}}{\tau^{\sigma}}} \tag{4}$$

where the momentum of the σ^{th} component is $\rho_\sigma u_\sigma = m_\sigma \sum f_i^{\sigma} e_i$, and $\boldsymbol{u}_\sigma$ is the macro velocity of σ^{th} component.

To simulate phase change, the potential force must be considered. For the pseudo potential model, the pseudo potential function is described [10]:

$$\mathbf{V}_{\sigma\bar{\sigma}}(\boldsymbol{x},\boldsymbol{x}') = G_{\sigma\bar{\sigma}}(\boldsymbol{x},\boldsymbol{x}')\phi_{\sigma}[f^{\sigma}(\boldsymbol{x})]\phi_{\bar{\sigma}}[f^{\bar{\sigma}}(\boldsymbol{x}')] \tag{5}$$

where $\phi_\sigma[f^{\sigma}(x)]$ and $\phi_{\bar{\sigma}}[f^{\bar{\sigma}}(x')]$ are the effective densities at position x for σ^{th} component and at $\boldsymbol{x}' = \boldsymbol{x} + \boldsymbol{e}_i$ for $\bar{\sigma}^{\mathrm{th}}$ component, respectively.

If only the isotropic interaction between neighboring nodes is considered, then Green function can be expressed:

$$G_{\sigma\bar{\sigma}}(\boldsymbol{x},\boldsymbol{x}') = \begin{cases} 0 & |\boldsymbol{x}-\boldsymbol{x}'| > \Delta x \\ G_{\sigma\bar{\sigma}} & |\boldsymbol{x}-\boldsymbol{x}'| \le \Delta x \end{cases} \tag{6}$$

where $G_{\sigma\bar{\sigma}}(\boldsymbol{x},\boldsymbol{x}') = G_{\bar{\sigma}\sigma}(\boldsymbol{x}',\boldsymbol{x})$, $\Delta\boldsymbol{x}$ – the lattice length, $G_{\sigma\bar{\sigma}}(\boldsymbol{x},\boldsymbol{x}')$ – the interaction strength between σ^{th} and $\bar{\sigma}^{\mathrm{th}}$ components, and the particle interactions of σ^{th} component can be taken:

$$\boldsymbol{F}_1(\boldsymbol{x}) = -\phi_{\sigma}[f^{\sigma}(\boldsymbol{x})]\sum_{x}\sum_{\sigma}G_{\sigma\bar{\sigma}}(\boldsymbol{x},\boldsymbol{x}')\phi_{\bar{\sigma}}[f^{\bar{\sigma}}(\boldsymbol{x}')](\boldsymbol{x}-\boldsymbol{x}') \tag{7}$$

When the fluid comes into contact with the solid phase, solid density remains the same and the force between fluids and solid walls at the fluid-solid interface is:

$$\boldsymbol{F}_2(\boldsymbol{x}) = -\phi_{\sigma}[f^{\sigma}(\boldsymbol{x})]\sum_{x}\sum_{\sigma}G_{\sigma w}(\boldsymbol{x},\boldsymbol{x}')\phi_{w}[f^{w}(\boldsymbol{x}')](\boldsymbol{x}-\boldsymbol{x}') \tag{8}$$

where $\phi_w[f^w(\boldsymbol{x}')]$ is the effective density of solid wall, and $\boldsymbol{x}'$ is a constant if it is on the solid surface, whereas the effective density is zero. Green function $G_{\sigma w}(\boldsymbol{x},\boldsymbol{x}')$ is the same as in eq. (7), but is characterized by the interaction intensity between fluids and solid walls, meanwhile, it can be used to reflect the soakage of fluid by adjusting the $G_{\sigma w}(\boldsymbol{x},\boldsymbol{x}')$.

Phase change model

This paper focuses on a simple ideal phase change process (other minor factors are ignored), and the basic assumptions are: calculation region reaches the saturation state, phase change rate is isotropic and has the same value in every discrete velocity directions, and to simulate phase change, heat flux, *q,* is supplied into the system. Based on the previous assumptions, a phase change term is introduced to simulate the phase change and two-phase LBM is used to prompt the bubble fusion and growth. Therefore, the basic phenomenon of boiling can be simulated, and the macroscopic mass transfer equation can be taken [11]:

$$\frac{\partial \rho_b V_b}{\partial t} = -\Theta_{b\to r}\rho_b V_b + \Theta_{r\to b}\rho_r V_r, \quad \frac{\partial \rho_r V_r}{\partial t} = \Theta_{b\to r}\rho_b V_b - \Theta_{r\to b}\rho_r V_r \tag{9}$$

where *b* and *r* are liquid and gas phases, respectively, ρ_b and ρ_r are the densities of liquid and gas phases, and V_b and V_r are volume fractions of liquid and gas phases, which satisfy $V_b + V_r = 1$. The, $\Theta_{b\to r}$, $\Theta_{r\to b}$ are phase change rates from liquid phase to gas phase and from gas phase to liquid phase, respectively.

This paper considers only the gasification process, hence eq. (9) can be simplified:

$$\frac{\partial \rho_b V_b}{\partial t} = -\Theta_{b\to r}\rho_b V_b, \quad \frac{\partial \rho_r V_r}{\partial t} = \Theta_{b\to r}\rho_b V_b \tag{10}$$

The change of two-phase volume fraction of gas and liquid over time during vaporization is:

$$V_b = 1 - \frac{1-\mathrm{e}^{-\Theta_{b\to r}t}}{1+(\gamma-1)\mathrm{e}^{-\Theta_{b\to r}t}}, \quad V_r = \frac{1-\mathrm{e}^{-\Theta_{b\to r}t}}{1+(\gamma-1)\mathrm{e}^{-\Theta_{b\to r}t}} \tag{11}$$

where γ denotes to density ratio of gas and liquid, the expression of mass of gas phase and liquid phase change over time is:

$$M_b = \rho_b V_b = M_{b0}\mathrm{e}^{-\Theta_{b\to r}t}, \quad M_r = \rho_r V_r = M_{b0}(1-\mathrm{e}^{-\Theta_{b\to r}t}) \tag{12}$$

where $M_{b0} = \rho_{b0}V_{b0}$ stands for initial quality of liquid phase, ρ_{b0} and V_{b0} are initial density and volume fraction of liquid phase, respectively. The densities of liquid and vapor in vaporization, ρ_b and ρ_r are:

$$\rho_b = \frac{\rho_{b0}[1+(\gamma-1)e^{-\Theta_{b\to r}t}]}{\gamma}, \quad \rho_r = \rho_{b0}[1+(\gamma-1)\mathrm{e}^{-\Theta_{b\to r}t}] \tag{13}$$

By introducing the mesoscopic phase change rate $\theta_{i,b\to r}$, $\theta_{i,b\to r} = \Theta_{b\to r}$ according to assumption (2). The phase change rate under constant temperature and pressure is associated with latent heat of gasification and it can be expressed:

$$\theta_{i,b\to r} = \Theta_{b\to r} = \frac{q}{h} \tag{14}$$

where *h* is the latent heat of evaporation, which is equal to 1.

Mesoscopic phase change equation is obtained [11]:

$$f_i^b = f_i^{b0} - \Theta_{b\to r} f_i^{b0}, \quad f_i^r = f_i^{r0} + \Theta_{b\to r} f_i^{r0} \tag{15}$$

where f_i^{b0} and f_i^{r0} are previous step distribution functions of the f_i^b and f_i^r.

Simulation of evaporation phase transition phenomenon

The phase change lattice Boltzmann model is applied to simulate the phase change process under isothermal condition when the superheat of system is 0.002. The simulation system has 200 × 200 lattice sites. At the initial time, the area was filled with liquid density $\rho_0 = 8.0$, and relaxation time $\tau = 1.0$, molecular weight $M_b = M_r = 1.0$, and interaction strength of fluids $G_{\sigma\bar{\sigma}}$=0.3. All of the physical quantities are dimensionless. Periodic boundary scheme is used for upper and lower boundaries, whereas bounce-back scheme is applied for the left and right boundaries. The interaction force of fluids and interaction force between fluids and walls are not considered. For the equation to evolve, the heat provides a disturbance of 1%, with computing iteration t for a total of 1000 steps. Figure 4 shows the vapor-liquid two-phase diagrams of pure liquid with different time steps. In this figure, the white part is the vapor, (*i. e.*, the formation of bubbles) and the black part is the liquid. Initially, some small bubbles begin to form in the region, and then the small bubbles continuously integrate into large bubbles. The hollow bubble rate in the whole area is increasing.

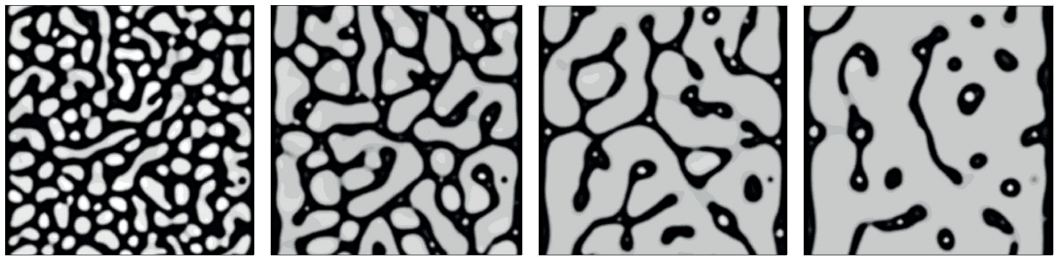

Figure 4. Two-phase distribution map with different time steps: (a) *t* = 300, (b) *t* = 500, (c) *t* = 800, and (d) *t* = 1000

Phase change Boltzmann model in porous media

Basic theory

For the phase change process in porous media, not only should the interaction force of fluid particles be considered, but also the interaction force between fluids and solid walls should be introduced into the Boltzmann model. As such, force term $\boldsymbol{F}_2$ is added on the basis of multiphase model mentioned in section *Basic multiphase model*. To achieve no-slip velocity boundary conditions, bounce-back format is applied for the collision of fluid and solid walls. The interaction force between fluids and solid walls can be express [12]:

$$\boldsymbol{F}_\sigma^s = -f^\sigma \sum_i G_{\sigma w} s(\boldsymbol{x} + \boldsymbol{e}_i)\boldsymbol{e}_i \tag{16}$$

The value of Boolean variable is either 0 (fluid lattice) or 1 (solid lattice), and it can describe the soakage (negative) and nonwetting (positive) of solids.

Analysis of simulation results

Figure 5 shows the random structure of reconstructed porous media. The porosity of this porous media is 0.6, P_c=0.01, P_5=P_7 = 0.05, and other directions P_i=0.005.

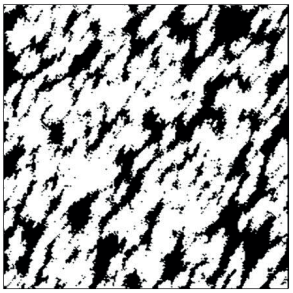

Figure 5. Reconstructed random porous media

The phase change lattice Boltzmann model of porous media is applied to 9 simulate the process of phase changing under isothermal condition and the superheat of system is 0.002. The simulation system is in a range of 200 × 200 lattice sites. Initially, the area was filled with liquid density $\rho_0 = 8.0$, relaxation time $\tau = 1.0$, molecular weight $M_b = M_r = 1.0$, interaction strength of fluids $G_{\sigma\sigma}$=0.3 and interaction force between fluids and solid walls is $G_{\sigma w}$=0.04. Periodic boundary scheme is used for all the four boundaries, whereas the internal solid boundaries are applied the bounce-back scheme. The interaction force of fluids was not considered. In order to make the equation to be evolving, the heat give a disturbance of 1%. Computing iteration t for a total of 1000 steps.

Figure 6 shows the vapor-liquid two-phase diagrams of pure liquid with different time steps of 300, 500, 800, and 1000 in porous media. In this figure, the white part is the solid skeleton, the black part is the liquid, and the gray part stands for gas phase. When the heat flux is supplied into the system, some small bubbles begin to form in the pores initially, and then the small bubbles continuously integrated into large bubbles. Effective collision and rebound process in porous media framework were also obtained. Finally, the bubbles almost occupied the entire pores.

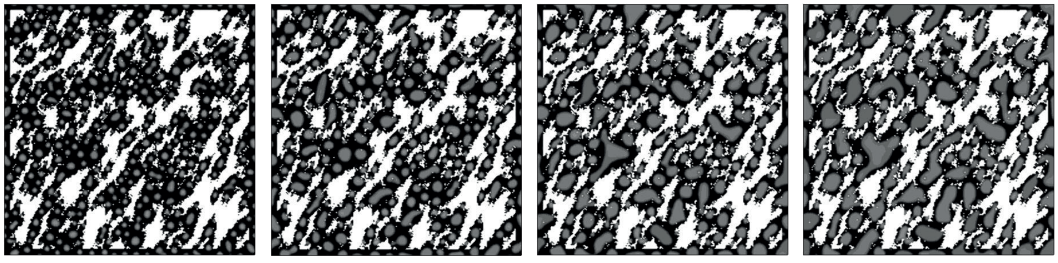

Figure 6. Two-phase distribution map with different time steps in random structures of porous media

Figure 7 shows the changes in volume of the (a) liquid and (b) gas phases in different superheat values in the process of evaporation. As we can see from the figure, the volume of liquid phase decreased, whereas the gas phase increased over time. Thus, in the process of phase change, the gas phase occupied the room of liquid phase gradually until the entire pores were fully occupied. At the same time, with the increase of superheat, the volume of gas phase is increase in the same time step, which means that the rate of phase change is as fast as the bubble growth.

Figure 8 shows the change of quality of the liquid and gas phases in different superheat values in the process of evaporation. The lines represent the theoretical results in eq. (12), whereas the discrete points represent the results of simulation. The calculation results show that in three different heat loads, the maximum relative errors between the qualities of gas phase and liquid phase and the theoretical solution for the gas phase are 0.09%, 0.19%, and 0.32%, respectively, whereas the values for the liquid phase are 0.11%, 0.38%, and 1.49%, respectively. The

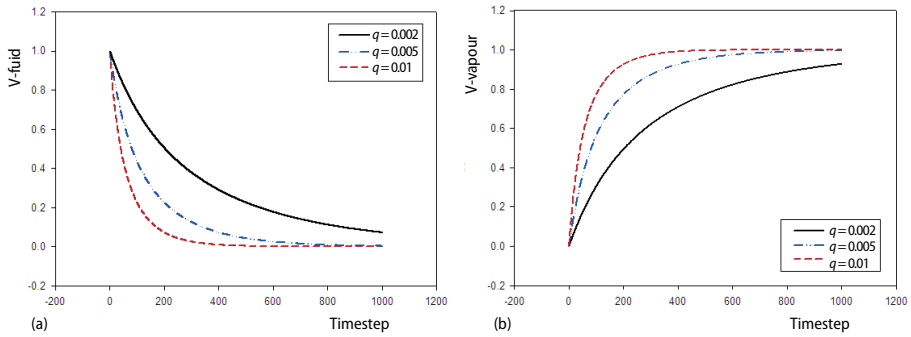

Figure 7. Changes in volume of (a) liquid and (b) gas phases in different superheat values

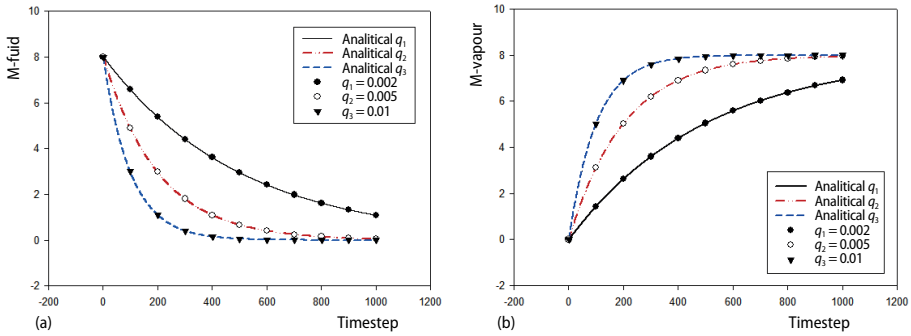

Figure 8. Change of quality of liquid (a) and gas (b) phase in different superheat

simulation results are consistent with the calculation results, verifying the accuracy of the model and the methods. With the increase in time step, the quantity of the liquid phase decreases gradually, by evaporation into gas phase. As a result, the quantity of the gas phase increases gradually.

Conclusion

At the pore scale level, 2-D porous medium structures of porous media was constructed using quartet structure generation set. A random porous cavity was selected and combined with the lattice Boltzmann model to describe the gas-liquid phase transition process. Following main conclusions can be achieved:

The porous media with different porosities (isotropic) and the same porosities (anisotropic) were constructed using quartet structure generation set. This method can effectively reconstruct the pore morphology and reflect the randomness of skeleton structure arrangement of rocks, foam metals and so on.

Analysis the transformation laws of liquid to gas in three different heat loads and results show that the maximum relative errors between the qualities of gas phase and liquid phase and the theoretical solution for the gas phase are 0.09%, 0.19% and 0.32%, respectively, whereas the values for the liquid phase are 0.11%, 0.38% and 1.49%, respectively. The simulation results are consistent with the calculation results

Combining the lattice Boltzmann model which can describe the gas-liquid phase transition process with reconstructed porous media, bubble generation, growth, mutual fusion and collision as well as rebound process in porous media framework were investigated by simulating the phase transition phenomenon in porous media. Simulation results coincide with the

theoretical solution perfectly, verifying the accuracy and feasibility of the model for random porous structures.

Acknowledgement

This work was supported by National Natural Science Foundation of China under Grant NO.51176069.

Nomenclature

h – latent heat of evaporation, [Jkg^{-1}]
T – dimensionless temperature, [–]
t – total step, [s]
V_b – volume fractions of liquid phase
V_r – volume fractions of gas phase
$\Theta_{r\to b}$ – phase change rates from gas phase to liquid phase, [kgs^{-1}]
ρ_b – densities of liquid phase, [kgm^{-3}]
ρ_r – densities of gas phase, [kgm^{-3}]
τ – dimensionless collision relaxation time

Greek Letters

γ – density ratio of gas and liquid, [kgm^{-3}]
ε – porosity of porous media
$\Theta_{b\to r}$ – phase change rates from liquid phase to gas phase, [kgs^{-1}]

Subscripts and superscripts

$b\to r$ – liquid phase to gas phase
i – nine directions
$r\to b$ – gas phase to liquid phase
σ – different components

References

[1] Liu, W., *et al.,* Heat and Mass Transfer with Phase Change in a Rectangular Enclosure Packed with Unsaturated Porous Material, *Heat and Mass Transfer*, *39* (2003), 3, pp. 223-230
[2] Huang, H. B., *et al.,* Evaluation of Three Lattice Boltzmann Models for Multiphase Flows in Porous Media, *Computers and Mathematics with Applications*, *61* (2011), 12, pp. 3606-3617
[3] Gao, D. Y., Chen, Z. Q., Lattice Boltzmann Simulation of Natural Convection Dominated Melting in a Rectangular Cavity Filled with Porous Media, *International Journal of Thermal Sciences*, *50* (2011), 4, pp. 493-501
[4] Omar, R. A., *et al.*, Numerical Simulation of Complete Liquid-Vapour Phase Change Process Inside Porous Media Using Smoothing of Diffusion Coefficient, *International Journal of Thermal Sciences*, *86* (2014), Dec., pp. 408-420
[5] He, Y. L., *et al.*, *Lattice Boltzmann Method: Theory and Applications*, Science Press, Beijing, 2009
[6] Xu, A.G., *et al*., Modeling and Simulation of Nonequilibrium and Multiphase Complex Systems-Lattice Boltzmann Kinetic Theory and Application, *Progress in Physics*, *34* (2014), Jan., pp. 136-163
[7] Zhao, K., *et al.*, Simulation of Phase Transition with Lattice Boltzmann Method (in Chinese), *Chinese Journal of Computational Physics*, *25* (2008), pp. 151-156
[8] Wang, M. R., *et al.*, Mesoscopic Predictions of the Effective Thermal Conductivity for Microscale Random Porous Media, *Phys. Rev. E., 47* (2007), Mar., pp. 036702
[9] Shan, X., Chen, H., Lattice Boltzmann Model for Simulating Flows with Multiple Phases and Components, *Phys. Rev. E., 47* (1993), 3, pp. 1815-1819
[10] Zeng, J. B., *et al*., Simulation of Boiling Process with Lattice Boltzmann Method, *Journal of Xi'an Jiaotong University*, *43* (2009), 7, pp. 25-29
[11] Kono, K., *et al.*, Application of Lattice Boltzmann Model to Multiphase Flows with Phase Transition, *Comput. Phys. Commun*., *129* (2000), 1-3, pp. 110-120
[12] Martys, N. S., Chen, H., Simulation of Multicomponent Fluids in Complex Three-Dimensional Geometries by the Lattice Boltzmann Method, *Phys. Rev., E., 53* (1996), 1, pp. 743-750

Paper submitted: August 17, 2016
Paper revised: November 28, 2016
Paper accepted: January 6, 2017